Effect of phosphorus addition on the MoS_2 phase morphology and performance of sulfided Mo/Al_2O_3 catalysts in HDO of rapeseed oil

EVGENIYA N. VLASOVA [a,b], VERA P. PAKHARUKOVA [a], GALINA A. BUKHTIYAROVA[a,b], IRINA V. DELIY [a,b], PAVEL V. ALEKSANDROV [a,b], ALEKSANDER A. PORSIN, EVGENY YU. GERASIMOV[a,b], VALERII V. BUKHTIYAROV[a,b]

[a] – Boreskov Institute of Catalysis SB RAS, 630090, Pr. Lavrentieva 5, Novosibirsk, RUSSIA.
[b] – Novosibirsk National Research University, 630090, Pirogova Street 2, Novosibirsk, RUSSIA
evgenia@catalysis.ru

Abstract: - The effect of phosphorus addition on the MoS_2 phase morphology and HDO activity was studied using catalysts, prepared without (MoS_2/Al_2O_3 catalyst) or with the addition ($P-MoS_2/Al_2O_3$ catalyst) of phosphoric acid to impregnation solution, initially containing MoO_3 and citric acid. Nearly the same average slab length of MoS_2 particles was determined with HRTEM on the surfaces of MoS_2/Al_2O_3 and $P-MoS_2/Al_2O_3$ catalysts. But the direct modeling of XRD patterns with using of the DSE gives the different average sizes of coherently scattering domains of the MoS_2 particles; with the lower d_{XRD} of the MoS_2 particles in the $P-MoS_2/Al_2O_3$ catalyst. A lower value of d_{XRD} in the case of $P-MoS_2/Al_2O_3$ catalyst seems to result from a higher degree of deformation of the supported MoS_2 particles, may be due to P incorporation in the MoS_2 slabs. Higher degree of deformation in turn could have been a reason of higher activity of $P-MoS_2/Al_2O_3$ catalyst in HDO and HDS reactions.

Key-Words: - hydrodeoxygenation, hydrodesulfurization, hydrotreatment, MoS_2, sulfide catalyst, co-processing, rapeseed oil

1 Introduction

The growing demand for transportation fuels along with the vital tendency to reduce the greenhouse gas emissions have stimulated the development of new catalysts for the production of liquid transportation fuels from the renewable resources. The hydroprocessing of triglyceride-based feedstock gives the mixture of alkanes, which are the valuable components for the improvement of the petroleum-based motor fuels properties [1]. The conventional hydrotreating sulphide $CoMo/Al_2O_3$ or $NiMo/Al_2O_3$ catalysts are widely used for the hydrodeoxygenation (HDO) of triglyceride-based feedstocks or their mixture with petroleum-derived fractions [2-10].

2 Problem Formulation

The HDO of triglycerides over sulfide $Co(Ni)Mo/Al_2O_3$ catalysts proceeds through the deoxygenation (with the water formation) or via decarbonylation/decarboxylation (with COx production) pathways, the latter route is highly undesirable because of ecological and technological reasons [2,3]. The non-promoted sulfide Mo/Al_2O_3 catalysts were shown to provide RSO conversion without considerable COx formation [11-13], that

makes them the promising candidates for the HDO of triglycerides. But the effects of precursors and preparation methods on the HDO activity were not studied in details. In our work the effect of phosphor addition to the impregnation solution on the state of the active phase and the performance of MoS_2/Al_2O_3 catalysts in HDO of rapeseed oil was investigated. Catalysts were prepared by an impregnation method with or without adding of phosphoric acid in the impregnation solution, prepared from MoO_3 and citric acid.

3 Problem Solution

3.1 Experimental

Mo/Al_2O_3 catalysts was prepared by impregnation of alumina granules (BET surface area 208 m^2 g^{-1}, pore volume 0.68 ml g^{-1}, average pore diameter 13,2 nm, purchased by JSK "Promkataliz", Ryazan, Russia) with a two different aqueous solution. The first solution was prepared using MoO_3 and citric acid; the second one contained MoO_3, citric acid and H_3PO_4 (all purchased by Vekton, Russia). The samples were denoted as MoS_2/Al_2O_3 and $P-MoS_2/Al_2O_3$, respectively. The catalysts were dried

in nitrogen flow at room temperature and then at 110°C for 4 h.

The textural properties of the catalysts were determined using nitrogen physisorption with an ASAP 2400 instrument (USA); the elemental analysis was performed using Optima 4300 DV (Perkin Elmer, France). The morphology of sulfide phase was studied using a JEM-2010 electron microscope (JEOL, Japan) with 1.4 Å lattice resolution at a 200 kV accelerating potential. Prior to the study, the samples were ground, suspended in ethanol and placed on a copper grid coated with a holey carbon film. XRD investigations were carried out at an ARL X'TRA diffractometer (Thermo, Switzerland) with a Si(Li) solid-state detector and Cu K_α radiation. The measurements were carried out in the 2θ range of 10°-80° with a step of 0.1°. Phase analysis was performed using the ICDD PDF-2 database.

The catalytic experiments were performed in a trickle-bed down-flow reactor with an inner diameter of 16 mm and length of 570 mm. In each experiment 10 ml of catalyst was diluted by an inert material, carborundum (0.1–0.25 mm size fraction) in a 1:2 volume ratio. The catalysts were examined after sulfidation with straight-run diesel fraction containing additionally 0.6 wt. % sulfur as dimethyl disulfide (at H_2 pressure 3.5 MPa; H/C – 300 Nm^3/m^3; LHSV- 2 hour^{-1}). The sulfidation was performed at 340°C during 6 h (heating rate was 25°C in hour). The catalytic experiments were performed at H_2 pressure 4.0 MPa, H/C – 600 Nm^3/m^3; LHSV – 1.5 h^{-1}, temperature – 260, 280, 300, 320 and 340°C; using mixture of 20 wt.% of rapeseed oil (RSO) diluted with straight run gas oil (SRGO). Properties of mixture were d = 0.86 g/cm^3, 2.34 wt. % O, 0.82 wt% S, 141 ppm N. The duration of each stages differing in temperature was 12 h; the residual sulfur and oxygen contents were obtained by averaging the data for three samples taken through 10, 11 and 12 h after the beginning of the current stage.

The sulfur content of the feedstock and that of the hydrogenated products were measured on a Lab-X 3500SCl energy dispersive X-ray fluorescence analyzer (Oxford Instruments, United Kingdom). The total oxygen content of the reaction mixture before and after hydrorefining was determined using a Vario EL Cube CHNSO analyzer (Elementar Analysensysteme GmbH, Germany).

The contents of C_{18} and C_{17} alkane (the products of RSO hydrodeoxygenation) in the products were evaluated using two-dimensional gas chromatography (Agilent 7890A GC equipped with a flame-ionization detector and an Agilent flow modulator). In the first dimension, separation was fulfilled using helium as carrier gas and ZB-WAX capillary column of 25 m long with a diameter of 0.25 mm and the film thickness of 0.25 μm (Phenomenex, United States). An HP-5 column of 5 m long and 0.25 mm in diameter with a film thickness of 0.25 μm (Agilent, United States) was used for the separation of components in the second dimension. The carrier gas was hydrogen. The conditions of chromatography were 70°C for 0.5 min, 8°C/min, and 260°C for 25 min. The flow through the first column was 0.5 mL/min (helium), while the flow through the second column was 31 mL/min (hydrogen). The period of modulation was 2.2 s. The volume of the introduced sample was 0.5 μL, and the split ratio was 1:200. The chromatographic data were processed with the ChemStation (Agilent) and Image GC (Zoex) software.

Gas phase was analyzed on-line using a gas chromatograph «Chromos 1000» (Dzerzhinsk, Russia), equipped with the FID detector. The concentrations of CO and CO_2 were determined in the form of methane after separation on column packed with 80/100 mesh HayeSep® («Sigma-Aldrich», St. Louis, MO, USA) and subsequent hydrogenation over reduced Pd catalyst at 340 °C.
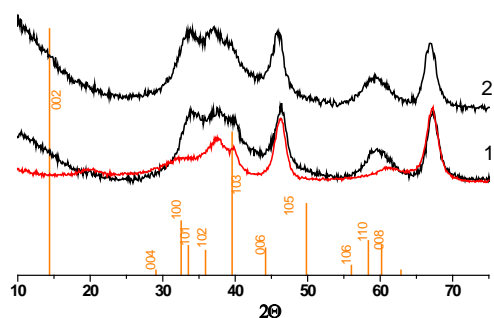
3.2 Results and discussion

Powder X-ray diffraction (XRD) analysis and high-resolution transmission electron microscopy (HRTEM) were used to study the structure and dispersion of the supported MoS_2 particles in the sulfide catalysts.

Low degree of crystallization of MoS_2 in hydroprocessing catalysts is known to limit application of traditional XRD methods for structure diagnostics. The Debye Function Analysis (DFA) was used to extract information on the structure of MoS_2 nanoparticles from the XRD data. The Debye Scattering Equation (DSE) allows calculating XRD pattern of model nanoparticle with taking into account the particle shape, size, chemical composition, and atomic structure [14-17]. Calculating and fitting XRD patterns were performed using the DIANNA software [18]. To evaluate an agreement between the calculated and experimental XRD profiles, a profile discrepancy factor (R_p).
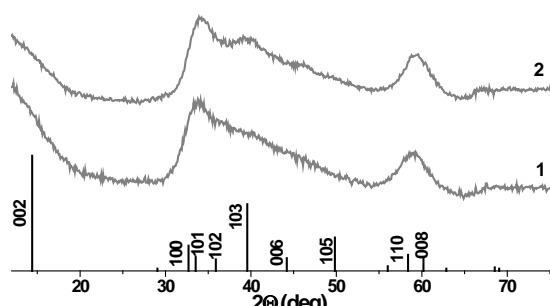
Fig.1 shows XRD patterns of the γ-Al_2O_3 support and MoS_2/ γ-Al_2O_3 catalysts. Highly broadened peaks in the 2θ ranges of 33-35° and 58-60° were detected in the XRD patterns of the catalysts, which

indicate formation of highly dispersed MoS_2 phase. Overlapping of the diffraction lines corresponding to the MoS_2 and γ-Al_2O_3 phases complicates the analysis.

Difference curves between the normalized XRD patterns of the catalyst and support were obtained to extract structural information on the MoS_2 nanoparticles (Fig.2).

Fig.1. XRD patterns of the P-MoS_2/Al_2O_3 (1) and MoS_2/Al_2O_3 (2) catalysts in comparison with XRD pattern of the $\gamma-Al_2O_3$ support. The peaks of the MoS_2 phase are shown.
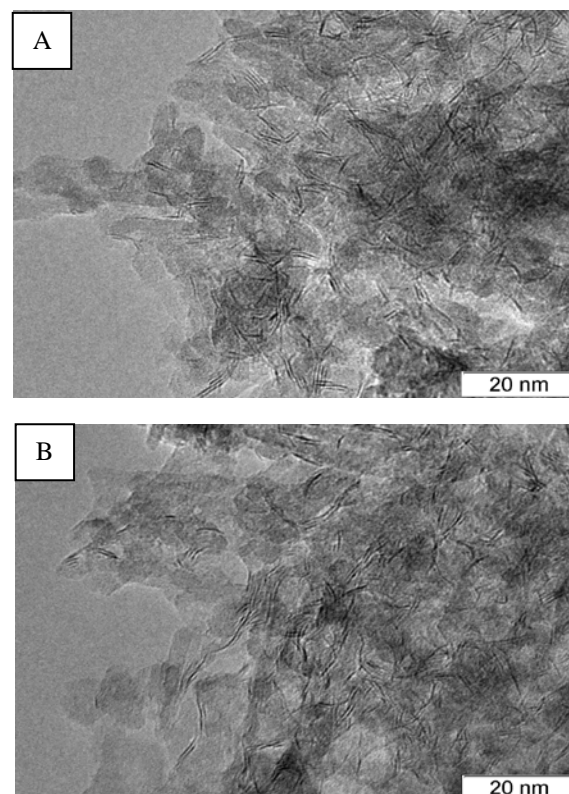

Fig.2. Difference XRD curves for the P-MoS_2/Al_2O_3 (1) and MoS_2/Al_2O_3 (2) catalysts

The formation of the poorly crystallized MoS_2 phase was revealed in the catalysts (JCPDS#37-1492, a=b=3.161 Å, c=12.299 Å, $\alpha=\beta=90°$, $\gamma=120°$). Disappearance of the first (002) reflection indicates the small size of coherently scattering domain (d_{XRD}) in the [001] direction, in which the skeletal MoS_2 layers are packed. HRTEM data also gave evidence of poor crystallization of the MoS_2 particles along the [001] direction (Fig.3). The average stacking number of 1.6 was determined in the both P-MoS_2/Al_2O_3 and MoS_2/Al_2O_3 catalysts (Table 1).

A direct modeling of XRD patterns with using the DSE was performed to determine the average size of coherently scattering domain. Starting from

one MoS_2 unit cell, a set of model plate-like crystallites was generated by varying lengths of the crystallite edges. The simulation of XRD data confirmed the absence of significant MoS_2 stacking in the P-MoS_2/Al_2O_3 and MoS_2/Al_2O_3 catalysts.
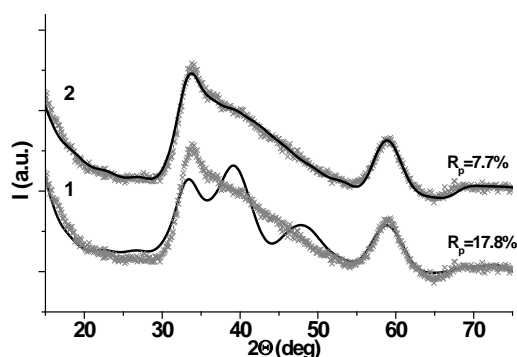

Fig.3. HRTEM images of the P-MoS_2/Al_2O_3 (A) and MoS_2/Al_2O_3 (B) catalysts

Table 1. Dispersion characteristics of MoS_2 particles in the sulfide catalysts from the XRD and HRTEM data

P-MoS_2/Al_2O_3		MoS_2/Al_2O_3	
average slab length of MoS_2 crystallites according to the XRD data modeling			
d_{XRD} (nm)	R_p (%)	d_{XRD} (nm)	R_p (%)
2.2x2.2	8.3	2.5x2.5	9.0
2.5x2.5	7.7	2.8x2.8	8.5
2.8x2.8	8.2	3.2x3.2	7.9
		3.5x3.5	7.8
		3.8x3.8	8.6
average slab length of MoS_2 particles according to the HRTEM data			
4.6		4.9	
average stacking number according to the HRTEM data			
1.6		1.6	

Fig.4 shows the experimental difference XRD curve of the P-MoS_2/Al_2O_3 catalyst in comparison with

calculated XRD patterns for the plate-like MoS_2 crystallites containing one and two MoS_2 layers with lateral dimensions of 2.5x2.5 nm (MoS_2 crystallites composed of 8x8x0.5 and 8x8x1 unit cells, respectively).

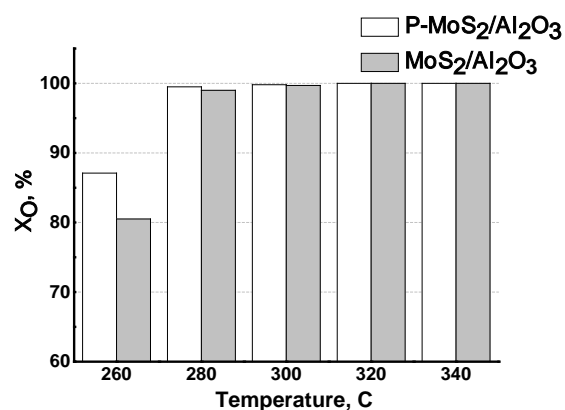
Fig.4. Experimental difference XRD curve of the P-MoS_2/Al_2O_3 catalyst and calculated XRD patterns for MoS_2 crystallites with dimensions of 2.5x2.5x1.2 nm (1) and 2.5x2.5x0.6 nm (2), containing one and two layers along the [001] direction, respectively.

The model of one-layer thick crystallites is more appropriate for describing the experimental XRD pattern. The calculated XRD pattern for the MoS_2 crystallites composed of two layers differs drastically from the experimental one. The lateral dimensions of MoS_2 crystallites of one-layer thickness (slab length) in the P-MoS_2/Al_2O_3 and MoS_2/Al_2O_3 catalysts were refined. The sizes d_{XRD} and corresponding discrepancy factors R_p are listed in Table 1.

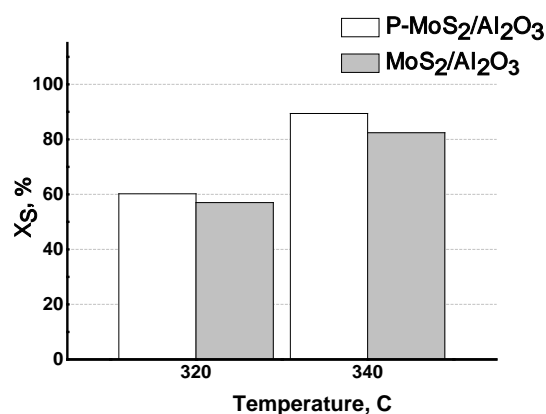The obtained data show that MoS_2 particles in the P-MoS_2/Al_2O_3 catalyst are characterized by a lower average size of coherently scattering domain d_{XRD}. The best fitting results were obtained at the slab sizes of 2.5 and 3.2-3.5 nm for P-MoS_2/Al_2O_3 and MoS_2/Al_2O_3 catalysts, respectively. A comparison of the particle sizes evaluated from XRD and HRTEM data shows a pronounced discrepancy. The dimensions of the coherent scattering domains determined from XRD data are significantly smaller than slab length of MoS_2 determined from HRTEM data (Table 1). The discrepancy is explained by deformation of MoS_2 particles, which leads to breaking coherence. Indeed, the MoS_2 sheets observed in the HRTEM images are curved or folded (Fig. 3). A lower value of d_{XRD} in the case of P-MoS_2/Al_2O_3 catalyst seems to result from a higher degree of deformation of the supported MoS_2 particles.

The results of catalytic testing of the MoS_2/Al_2O_3 and P-MoS_2/Al_2O_3 catalysts in the hydrotreating of RSO/SRGO mixture are presented in the Fig.5-6. Degree of RSO hydrodeoxygenation (Fig.5) was

calculated using oxygen content in the raw material (mixture of RSO with SRGO) and in the liquid products measured by means of Vario EL Cube analyzer. The RSO conversion achieved 100% at 320 and 340°C over both catalysts; but P-MoS_2/Al_2O_3 catalyst demonstrated higher HDO activity at 260, 280 and 300°C (Fig.5). P-MoS_2/Al_2O_3 catalyst as well displayed higher activity in HDS of SRGO in comparison with MoS_2/Al_2O_3 catalyst in the whole temperature range (Fig.6).

Fig.5. Hydrodeoxygenation activity of P-MoS_2/Al_2O_3 and MoS_2/Al_2O_3 catalysts at different temperatures

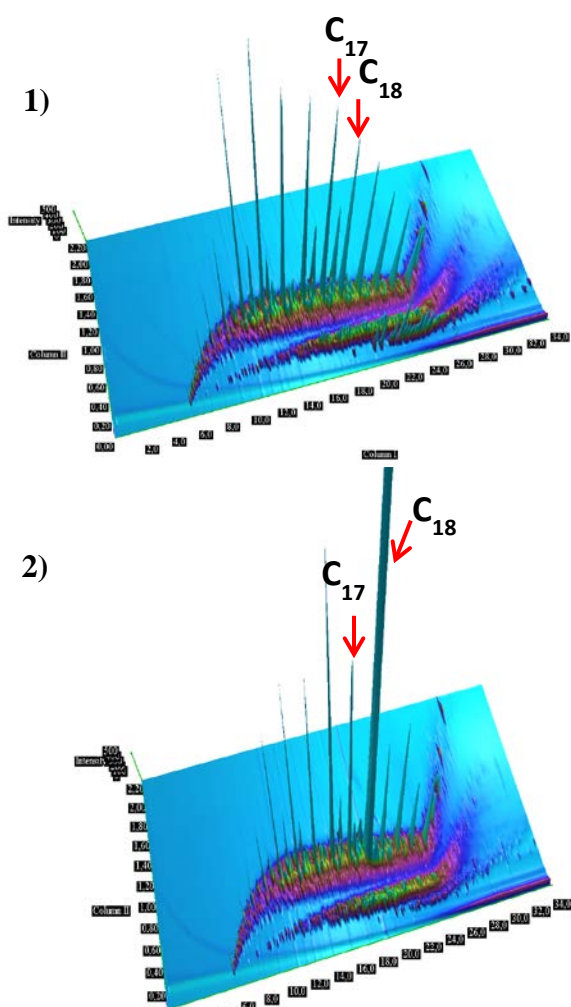**Fig.6.** Hydrodesulfurization activity of P-MoS_2/Al_2O_3 and MoS_2/Al_2O_3 catalysts at 320 and 340°C

The selectivity of RSO conversion through HDO or $HDeCO_x$ pathways was evaluated taking gas phase analysis and the results of C_{18} and C_{17} content measurement by means of two-dimensional chromatography.

The typical chromatograms of SRGO and reaction products, obtained during HDO of RSO/SRGO mixture over MoS_2 at 340°C is presented in Fig.7. The quantitative analysis of C_{18} and C_{17} in the reaction products and in the SRGO let

us to calculate the selectivity of octadecane formation that lies within the region 97-99% for both catalysts at whole conversion of RSO (at 320 and 340°C).

The results of CO_x analysis in the exit gas flow confirmed the high selectivity of RSO hydrodeoxygenation though the "direct" HDO route over both catalysts. CO_x content was negligible at 260°C (about 0.04 vol.%) and slightly increased (up to 0.10-0.12 vol.%), with the temperature raising from 260 to 340°C. But the selectivity of $DeCO_x$ pathway calculated from the gas phase analysis did not exceed 3.0% even at 340°C.

Fig.7. 2D-chromatograms of straight run gas oil (1) and the product obtained (2) in presence of P-MoS_2/Al_2O_3 at 340°C

4 Conclusion

The effect of phosphorus addition on the morphology of MoS_2 phase and catalytic performance of sulfide Mo/Al_2O_3 catalysts in the HDO of rapeseed oil was studied using two different

impregnating solutions for preparation of the catalysts. MoS_2/Al_2O_3 catalyst was obtained from solution prepared using MoO_3 and citric acid; the solution prepared from MoO_3, citric acid and H_3PO_4 was used for the P-MoS_2/Al_2O_3 catalyst preparation. The thorough investigation of the sulfide MoS_2/Al_2O_3 and P-MoS_2/Al_2O_3 catalysts with XRD and HRTEM methods led us to conclusion, that despite nearly the same average slab length of MoS_2 particles determined with HRTEM on the surfaces of both catalysts, the MoS_2 particles in the P-MoS_2/Al_2O_3 catalysts are characterized by a lower average size of coherently scattering domain d_{XRD}. A lower value of d_{XRD} in the case of P-MoS_2/Al_2O_3 catalyst seems to result from a higher degree of deformation of the supported MoS_2 particles, maybe due to P incorporation in the MoS_2 slabs. Higher degree of deformation in turn could have been a reason of higher activity of P-MoS_2/Al_2O_3 catalyst in HDO and HDS reactions.

References:

[1] Al-Sabawi M., Chen J., Hydroprocessing of biomass-derived oils and their blends with petroleum feedstocks: a review, *Energy & Fuels*, Vol.26, №9, 2012, pp. 5373-5399.

[2] Furimsky E., Hydroprocessing challenges in biofuels production, *Catalysis Today*, Vol.217, 2013, pp. 13-56.

[3] Kubicka D., Tucas V. *Advances in Chemical Engeneering*, Elsevier, Vol.42, 2013.

[4] Mohammad M., Hari T. K., Yaakob Z., Sharma Y. C., Sopian K., Overview on the production of paraffin based-biofuels via catalytic hydrodeoxygenation, *Renewable and Sustainable Energy Reviews*. Vol.22, 2013, pp. 121-132.

[5] Satyarthi J.K., Chiranjeevi T., Gokak D.T., Viswanathan P.S., An overview of catalytic conversion of vegetable oils/fats into middle distillates, *Catalysis Science & Technology*, Vol.3, 2013, pp. 70-80.

[6] Nikul'shin P., Sal'nikov V., Pimerzin A., Eremina Y., Koklyukhin A., Tsvetkov V., Pimerzin A., Co-hydrotreating of straight-run diesel fraction and vegetable oil on Co(Ni)-PMo/Al₂O₃ catalysts , *Petroleum Chemistry*, Vol.56, №1, 2016, pp. 56-61.

[7] Vlasova E. N., Deliy I. V., Nuzhdin A. L., Aleksandrov P. V., Gerasimov E. Y., Aleshina, G. I., Bukhtiyarova, G. A., Catalytic properties of CoMo/Al₂O₃ sulfide catalysts in the hydrorefining of straight-run diesel fraction mixed with rapeseed oil, *Kinetics and Catalysis*, Vol.55. №4, 2014, pp. 481-491

[8] Anthonykutty J. M., Linnekoski J. et al., Catalytic upgrading of crude tall oil into a paraffin-rich liquid, *Biomass Conversion and Biorefinery*, Vol.5, №2, 2015, pp. 149-159.

[9] Tóth C., Baladincz P., Hancsók J, Production of biocomponent containing gas oil with the coprocessing of vegetable oil–gas oil mixture, *Topics in Catalysis*, Vol.54, №16-18, 2011, pp. 1084-1093.

[10] Srifa A., Faungnawakij K. et al., Production of bio-hydrogenated diesel by catalytic hydrotreating of palm oil over NiMoS₂/gamma-Al₂O₃ catalyst, *Bioresource Technology,* Vol.158, 2014, pp. 81-90.

[11] Kubicka D., Kaluza L., Deoxygenation of vegetable oils over sulfided Ni, Mo and NiMo catalysts, *Applied Catalysis A: General*, Vol.372, №2, 2010, pp. 199-208.

[12] De Brimont M. R. et al., Deoxygenation mechanisms on Ni-promoted MoS₂ bulk catalysts: a combined experimental and theoretical study, *Journal of Catalysis,* Vol.286, 2012, pp. 153-164.

[13] Deliy I. V. et al., Hydrodeoxygenation of methyl palmitate over sulfided Mo/Al₂O₃, CoMo/Al₂O₃ and NiMo/Al₂O₃ catalysts, *RSC Advances*, Vol.4, №5, 2014, pp. 2242-2250.

[14] Debye P., Scattering from non-crystalline substances, *Ann. Physik.*, Vol. 46, 1915, pp. 809-823.

[15] Guinier A., *X-ray Diffraction in Crystals, Imperfect Crystals and Amorphous Bodies*, Dover, New York, 1994.

[16] Hall B. D., Debye function analysis of structure in diffraction from nanometer-sized particles, *Journal of Applied Physics*, Vol.87, №4, 2000, pp. 1666-1675.

[17] Tsybulya S. V., Yatsenko D. A., X-ray diffraction analysis of ultradisperse systems: The Debye formula, *Journal of Structural Chemistry*, Vol.53, №1, 2012, pp. 150-165.

[18] Yatsenko D. A., Tsybulya S. V., DIANNA (Diffraction Analysis of Nanopowders): Software for structural analysis of ultradisperse systems by X-Ray methods, *Bulletin of the Russian Academy of Sciences: Physics*., Vol.76, №3, 2012, pp. 382-384.